Measurement of the Transverse Single-Spin Asymmetry in $p^{\uparrow} + p \to W^{\pm}/Z^{0}$ at RHIC

L. Adamczyk,[1] J. K. Adkins,[20] G. Agakishiev,[18] M. M. Aggarwal,[31] Z. Ahammed,[49] I. Alekseev,[16] A. Aparin,[18] D. Arkhipkin,[3] E. C. Aschenauer,[3] A. Attri,[31] G. S. Averichev,[18] X. Bai,[7] V. Bairathi,[27] A. Banerjee,[49] R. Bellwied,[45] A. Bhasin,[17] A. K. Bhati,[31] P. Bhattarai,[44] J. Bielcik,[10] J. Bielcikova,[11] L. C. Bland,[3] I. G. Bordyuzhin,[16] J. Bouchet,[19] J. D. Brandenburg,[37] A. V. Brandin,[26] I. Bunzarov,[18] J. Butterworth,[37] H. Caines,[53] M. Calderón de la Barca Sánchez,[5] J. M. Campbell,[29] D. Cebra,[5] I. Chakaberia,[3] P. Chaloupka,[10] Z. Chang,[43] S. Chattopadhyay,[49] X. Chen,[22] J. H. Chen,[40] J. Cheng,[46] M. Cherney,[9] W. Christie,[3] G. Contin,[23] H. J. Crawford,[4] S. Das,[13] L. C. De Silva,[9] R. R. Debbe,[3] T. G. Dedovich,[18] J. Deng,[39] A. A. Derevschikov,[33] B. di Ruzza,[3] L. Didenko,[3] C. Dilks,[32] X. Dong,[23] J. L. Drachenberg,[48] J. E. Draper,[5] C. M. Du,[22] L. E. Dunkelberger,[6] J. C. Dunlop,[3] L. G. Efimov,[18] J. Engelage,[4] G. Eppley,[37] R. Esha,[6] O. Evdokimov,[8] O. Eyser,[3] R. Fatemi,[20] S. Fazio,[3] P. Federic,[11] J. Fedorisin,[18] Z. Feng,[7] P. Filip,[18] Y. Fisyak,[3] C. E. Flores,[5] L. Fulek,[1] C. A. Gagliardi,[43] D. Garand,[34] F. Geurts,[37] A. Gibson,[48] M. Girard,[50] L. Greiner,[23] D. Grosnick,[48] D. S. Gunarathne,[42] Y. Guo,[38] A. Gupta,[17] S. Gupta,[17] W. Guryn,[3] A. Hamad,[19] A. Hamed,[43] R. Haque,[27] J. W. Harris,[53] L. He,[34] S. Heppelmann,[32] S. Heppelmann,[5] A. Hirsch,[34] G. W. Hoffmann,[44] D. J. Hofman,[8] S. Horvat,[53] X. Huang,[46] H. Z. Huang,[6] B. Huang,[8] T. Huang,[28] P. Huck,[7] T. J. Humanic,[29] G. Igo,[6] W. W. Jacobs,[15] H. Jang,[21] A. Jentsch,[44] J. Jia,[3] K. Jiang,[38] E. G. Judd,[4] S. Kabana,[19] D. Kalinkin,[15] K. Kang,[46] K. Kauder,[51] H. W. Ke,[3] D. Keane,[19] A. Kechechyan,[18] Z. H. Khan,[8] D. P. Kikoła,[50] I. Kisel,[12] A. Kisiel,[50] L. Kochenda,[26] D. D. Koetke,[48] L. K. Kosarzewski,[50] A. F. Kraishan,[42] P. Kravtsov,[26] K. Krueger,[2] L. Kumar,[31] M. A. C. Lamont,[3] J. M. Landgraf,[3] K. D. Landry,[6] J. Lauret,[3] A. Lebedev,[3] R. Lednicky,[18] J. H. Lee,[3] C. Li,[38] Y. Li,[46] W. Li,[40] X. Li,[38] X. Li,[42] T. Lin,[15] M. A. Lisa,[29] F. Liu,[7] T. Ljubicic,[3] W. J. Llope,[51] M. Lomnitz,[19] R. S. Longacre,[3] X. Luo,[7] R. Ma,[3] L. Ma,[40] G. L. Ma,[40] Y. G. Ma,[40] N. Magdy,[41] R. Majka,[53] A. Manion,[23] S. Margetis,[19] C. Markert,[44] D. McDonald,[45] K. Meehan,[5] J. C. Mei,[39] N. G. Minaev,[33] S. Mioduszewski,[43] D. Mishra,[27] B. Mohanty,[27] M. M. Mondal,[43] D. A. Morozov,[33] M. K. Mustafa,[23] B. K. Nandi,[14] Md. Nasim,[6] T. K. Nayak,[49] G. Nigmatkulov,[26] T. Niida,[51] L. V. Nogach,[33] S. Y. Noh,[21] J. Novak,[25] S. B. Nurushev,[33] G. Odyniec,[23] A. Ogawa,[3] K. Oh,[35] V. A. Okorokov,[26] D. Olvitt, Jr.,[42] B. S. Page,[3] R. Pak,[3] Y. X. Pan,[6] Y. Pandit,[8] Y. Panebratsev,[18] B. Pawlik,[30] H. Pei,[7] C. Perkins,[4] P. Pile,[3] J. Pluta,[50] K. Poniatowska,[50] J. Porter,[23] M. Posik,[42] A. M. Poskanzer,[23] N. K. Pruthi,[31] J. Putschke,[51] H. Qiu,[23] A. Quintero,[19] S. Ramachandran,[20] R. Raniwala,[36] S. Raniwala,[36] R. L. Ray,[44] H. G. Ritter,[23] J. B. Roberts,[37] O. V. Rogachevskiy,[18] J. L. Romero,[5] A. Roy,[49] L. Ruan,[3] J. Rusnak,[11] O. Rusnakova,[10] N. R. Sahoo,[43] P. K. Sahu,[13] I. Sakrejda,[23] S. Salur,[23] J. Sandweiss,[53] A. Sarkar,[14] J. Schambach,[44] R. P. Scharenberg,[34] A. M. Schmah,[23] W. B. Schmidke,[3] N. Schmitz,[24] J. Seger,[9] P. Seyboth,[24] N. Shah,[40] E. Shahaliev,[18] P. V. Shanmuganathan,[19] M. Shao,[38] M. K. Sharma,[17] B. Sharma,[31] W. Q. Shen,[40] Z. Shi,[23] S. S. Shi,[7] Q. Y. Shou,[40] E. P. Sichtermann,[23] R. Sikora,[1] M. Simko,[11] S. Singha,[19] M. J. Skoby,[15] D. Smirnov,[3] N. Smirnov,[53] W. Solyst,[15] L. Song,[45] P. Sorensen,[3] H. M. Spinka,[2] B. Srivastava,[34] T. D. S. Stanislaus,[48] M. Stepanov,[34] R. Stock,[12] M. Strikhanov,[26] B. Stringfellow,[34] M. Sumbera,[11] B. Summa,[32] Y. Sun,[38] Z. Sun,[22] X. M. Sun,[7] B. Surrow,[42] D. N. Svirida,[16] A. H. Tang,[3] Z. Tang,[38] T. Tarnowsky,[25] A. Tawfik,[52] J. Thäder,[23] J. H. Thomas,[23] A. R. Timmins,[45] D. Tlusty,[37] T. Todoroki,[3] M. Tokarev,[18] S. Trentalange,[6] R. E. Tribble,[43] P. Tribedy,[3] S. K. Tripathy,[13] O. D. Tsai,[6] T. Ullrich,[3] D. G. Underwood,[2] I. Upsal,[29] G. Van Buren,[3] G. van Nieuwenhuizen,[3] M. Vandenbroucke,[42] R. Varma,[14] A. N. Vasiliev,[33] R. Vertesi,[11] F. Videbæk,[3] S. Vokal,[18] S. A. Voloshin,[51] A. Vossen,[15] J. S. Wang,[22] Y. Wang,[46] F. Wang,[34] Y. Wang,[7] H. Wang,[3] G. Wang,[6] J. C. Webb,[3] G. Webb,[3] L. Wen,[6] G. D. Westfall,[25] H. Wieman,[23] S. W. Wissink,[15] R. Witt,[47] Y. Wu,[19] Z. G. Xiao,[46] X. Xie,[38] W. Xie,[34] K. Xin,[37] N. Xu,[23] Y. F. Xu,[40] Z. Xu,[3] Q. H. Xu,[39] J. Xu,[7] H. Xu,[22] Q. Yang,[38] Y. Yang,[28] S. Yang,[38] Y. Yang,[22] C. Yang,[38] Y. Yang,[7] Z. Ye,[8] Z. Ye,[8] P. Yepes,[37] L. Yi,[53] K. Yip,[3] I.-K. Yoo,[35] N. Yu,[7] H. Zbroszczyk,[50] W. Zha,[38] S. Zhang,[40] Z. Zhang,[40] S. Zhang,[38] J. B. Zhang,[7] Y. Zhang,[38] J. Zhang,[39] J. Zhang,[22] X. P. Zhang,[46] J. Zhao,[34] C. Zhong,[40] L. Zhou,[38] X. Zhu,[46] Y. Zoulkarneeva,[18] and M. Zyzak[12]

(STAR Collaboration)

[1]*AGH University of Science and Technology, FPACS, Cracow 30-059, Poland*
[2]*Argonne National Laboratory, Argonne, Illinois 60439*
[3]*Brookhaven National Laboratory, Upton, New York 11973*
[4]*University of California, Berkeley, California 94720*
[5]*University of California, Davis, California 95616*
[6]*University of California, Los Angeles, California 90095*

[7]Central China Normal University, Wuhan, Hubei 430079
[8]University of Illinois at Chicago, Chicago, Illinois 60607
[9]Creighton University, Omaha, Nebraska 68178
[10]Czech Technical University in Prague, FNSPE, Prague 115 19, Czech Republic
[11]Nuclear Physics Institute AS CR, 250 68 Prague, Czech Republic
[12]Frankfurt Institute for Advanced Studies FIAS, Frankfurt 60438, Germany
[13]Institute of Physics, Bhubaneswar 751005, India
[14]Indian Institute of Technology, Mumbai 400076, India
[15]Indiana University, Bloomington, Indiana 47408
[16]Alikhanov Institute for Theoretical and Experimental Physics, Moscow 117218, Russia
[17]University of Jammu, Jammu 180001, India
[18]Joint Institute for Nuclear Research, Dubna 141 980, Russia
[19]Kent State University, Kent, Ohio 44242
[20]University of Kentucky, Lexington, Kentucky 40506-0055
[21]Korea Institute of Science and Technology Information, Daejeon 305-701, Korea
[22]Institute of Modern Physics, Chinese Academy of Sciences, Lanzhou, Gansu 730000
[23]Lawrence Berkeley National Laboratory, Berkeley, California 94720
[24]Max-Planck-Institut für Physik, Munich 80805, Germany
[25]Michigan State University, East Lansing, Michigan 48824
[26]National Research Nuclear University MEPhI, Moscow 115409, Russia
[27]National Institute of Science Education and Research, Bhubaneswar 751005, India
[28]National Cheng Kung University, Tainan 70101
[29]Ohio State University, Columbus, Ohio 43210
[30]Institute of Nuclear Physics PAN, Cracow 31-342, Poland
[31]Panjab University, Chandigarh 160014, India
[32]Pennsylvania State University, University Park, Pennsylvania 16802
[33]Institute of High Energy Physics, Protvino 142281, Russia
[34]Purdue University, West Lafayette, Indiana 47907
[35]Pusan National University, Pusan 46241, Korea
[36]University of Rajasthan, Jaipur 302004, India
[37]Rice University, Houston, Texas 77251
[38]University of Science and Technology of China, Hefei, Anhui 230026
[39]Shandong University, Jinan, Shandong 250100
[40]Shanghai Institute of Applied Physics, Chinese Academy of Sciences, Shanghai 201800
[41]State University of New York, Stony Brook, New York 11794
[42]Temple University, Philadelphia, Pennsylvania 19122
[43]Texas A&M University, College Station, Texas 77843
[44]University of Texas, Austin, Texas 78712
[45]University of Houston, Houston, Texas 77204
[46]Tsinghua University, Beijing 100084
[47]United States Naval Academy, Annapolis, Maryland 21402
[48]Valparaiso University, Valparaiso, Indiana 46383
[49]Variable Energy Cyclotron Centre, Kolkata 700064, India
[50]Warsaw University of Technology, Warsaw 00-661, Poland
[51]Wayne State University, Detroit, Michigan 48201
[52]World Laboratory for Cosmology and Particle Physics (WLCAPP), Cairo 11571, Egypt
[53]Yale University, New Haven, Connecticut 06520

(Received 20 November 2015; published 1 April 2016)

We present the measurement of the transverse single-spin asymmetry of weak boson production in transversely polarized proton-proton collisions at $\sqrt{s} = 500$ GeV by the STAR experiment at RHIC. The measured observable is sensitive to the Sivers function, one of the transverse-momentum-dependent parton distribution functions, which is predicted to have the opposite sign in proton-proton collisions from that observed in deep inelastic lepton-proton scattering. These data provide the first experimental investigation of the nonuniversality of the Sivers function, fundamental to our understanding of QCD.

DOI: 10.1103/PhysRevLett.116.132301

During the past decade there have been tremendous efforts towards understanding the three-dimensional partonic structure of the proton. One way to describe the $2+1$ dimensional structure of the proton in momentum space is via transverse-momentum-dependent parton distribution functions (TMDs) [1], which encode a dependence on the intrinsic transverse momentum of the parton k_T, in addition to the longitudinal momentum fraction x of the parent proton carried by the parton. There are eight TMDs that are allowed by parity invariance [2]. Of particular interest is the Sivers function [3], $f_{1T}^{\perp}$, which describes the correlation between the intrinsic transverse momentum of a parton and the spin of the parent proton. It may be described as the parton density of the vector structure $(\vec{P} \times \vec{k}_T) \cdot \vec{S}$, where $\vec{P}$ and $\vec{S}$ are the proton momentum and the spin vectors, respectively. In $p+p$ collisions in which one of the proton beams is transversely polarized, the Sivers function can be accessed through measurements of the transverse single-spin asymmetry (TSSA) in Drell-Yan (DY) or $W^{\pm}/Z^0$ boson production, which is defined as $(\sigma_{\uparrow} - \sigma_{\downarrow})/(\sigma_{\uparrow} + \sigma_{\downarrow})$, where $\sigma_{\uparrow(\downarrow)}$ is the cross section measured with the spin direction of the proton beam pointing up (down).

In addition to providing access to the three-dimensional structure of the nucleon, there are nontrivial predictions for the process dependence of the Sivers function stemming from gauge invariance. In semi-inclusive deep inelastic scattering (SIDIS), the Sivers function is associated with a final-state effect through gluon exchange between the struck parton and the target nucleon remnants [4]. In $p+p$ collisions, on the other hand, the Sivers asymmetry originates from the initial state of the interaction for the DY process and $W^{\pm}/Z^0$ boson production. As a consequence, the gauge invariant definition of the Sivers function predicts the opposite sign for the Sivers function in SIDIS compared to processes with color charges in the initial state and a colorless final state, such as $p+p \to \mathrm{DY}/W^{\pm}/Z^0$ [5]:

$$f_{q/h^{\uparrow}}^{\mathrm{SIDIS}}(x, k_T, Q^2) = -f_{q/h^{\uparrow}}^{p+p \to \mathrm{DY}/W^{\pm}/Z^0}(x, k_T, Q^2). \quad (1)$$

This nonuniversality of the Sivers function is a fundamental prediction from the gauge invariance of the theory of quantum chromodynamics (QCD) and is based on the QCD factorization formalism [5,6]. The experimental test of this sign change is a crucial measurement in hadronic physics [7], and it will provide an important test of our understanding of QCD factorization.

DY and $W^{\pm}$, Z^0 production in $p+p$ collisions provides the two scales required to apply the TMD framework to transverse single-spin asymmetries. A hard scale is given by the photon virtuality (Q^2) or by the mass of the produced boson ($M^2 \sim Q^2$), while a soft scale of the order of the intrinsic k_T is given by the transverse momentum. While a measurement of the TSSA in Drell-Yan production at forward pseudorapidities ($\eta > 3$) is experimentally very challenging, requiring severe background suppression and substantial integrated luminosity, a TSSA measurement in weak boson production offers several unique advantages. Because of the high $Q^2 \simeq M_{W/Z}^2$ scale provided by the large boson mass ($M_{W/Z}$), the measurement of the TSSA amplitude (A_N) in weak boson production provides a stringent test of the evolution of the TMDs [8], which, as with other asymmetries, are expected to partially cancel in the ratio of polarized to unpolarized cross sections. The rapidity dependence of A_N for the $W^+(W^-)$ boson, which is produced through $u + \bar{d}(d + \bar{u})$ fusion, provides an essential input to reduce the uncertainty on the Sivers function for light sea quarks. That Sivers function, determined by fits to SIDIS data [8] in a Bjorken-x range where the asymmetry of the $\bar{u}$ and $\bar{d}$ unpolarized sea quark densities [9] can only be explained by strong nonperturbative QCD contributions, is essentially unconstrained.

The A_N of the lepton produced in $W^{\pm}$ decay is predicted [10,11] to vary rapidly with the lepton kinematics, having a nonzero value in only a narrow region in lepton transverse momentum and pseudorapidity. On the other hand, the asymmetry is predicted to have a sizable value over a large range of the produced boson kinematics [11], its actual magnitude depending on the TMD evolution [8]. Therefore, in measuring A_N, it is preferable to fully reconstruct the W boson.

In this Letter, we report the measurement of A_N for weak bosons in proton-proton collisions at $\sqrt{s} = 500$ GeV with transversely polarized beams by the STAR experiment at RHIC. The data sample used in this analysis was collected in 2011 and corresponds to a recorded integrated luminosity of 25 pb^{-1}. The beam polarization was measured using Coulomb-nuclear interference proton-carbon polarimeters, calibrated with a polarized hydrogen gas-jet target. The average beam polarization for the data set used in the present analysis was 53%, with a relative scale uncertainty of $\Delta P/P = 3.4\%$ [12]. The subsystems of the STAR detector [13] used in this measurement are the time projection chamber (TPC) [14], providing charged particle tracking for pseudorapidity $|\eta| \leq 1.3$, and the barrel electromagnetic calorimeter (BEMC) [15], covering the full azimuthal angle ϕ for $|\eta| < 1$.

In this analysis, data were recorded using a calorimeter trigger requirement of 12 GeV of transverse energy E_T in a $\Delta\eta \times \Delta\phi$ region of $\sim 0.1 \times 0.1$ of the BEMC. Based on previous STAR analyses of weak boson longitudinal spin asymmetries [16] and cross sections [17], we selected a data sample characterized by the $W \to e\nu$ signature, requiring an isolated electron with $P_T^e > 25$ GeV/c within the BEMC acceptance ($|\eta| < 1$). In reconstructing the momentum of the decay electron, its energy was measured in the BEMC and its trajectory using the TPC.

To ensure the isolation of the decay electron, it is required that the ratio of the sum of the electron momentum

and energy, $(P^e + E^e)$, over the sum of the momenta and energies of all of the particles contained in a cone with a radius $R = \sqrt{(\eta^2 + \phi^2)} = 0.7$ around the decay electron track, $\Sigma_{R\text{cone}=0.7}[P^{\text{tracks}} + E^{\text{cluster}}]$, must be larger than 0.9. All tracks must come from a single vertex with $|Z_{\text{vertex}}| < 100$ cm.

We define the variable P_T-balance, $\vec{P}_T^{\text{bal}}$, as the vector sum of the decay electron candidate $\vec{P}_T^{e}$ and the transverse momentum of the hadronic recoil, $\vec{P}_T^{\text{recoil}}$. The latter is calculated as the vector sum of the transverse momenta of all tracks with $P_T > 200$ MeV/c, excluding the decay electron candidate, and the E_T of all clusters in the BEMC without a matching track and with an energy above the noise threshold of 200 MeV. In order to reject QCD background events, the scalar variable $(\vec{P}_T^{\text{bal}} \cdot \vec{P}_T^{e})/|\vec{P}_T^{e}|$ is required to be larger than 18 GeV/c.

After applying all of the selection criteria, the remaining electron candidates are sorted by charge. Charge misidentification was minimized by requiring that the lepton transverse momentum, $P_T^{e\text{-track}}$, as measured by the TPC track, satisfies the condition $0.4 < E_T^e/P_T^{e\text{-track}} < 1.8$ for both charge signs. The contamination from incorrectly assigned events is estimated to be ~0.004%. The selection yields final data samples of 1016 W^+ events and 275 W^- events for 0.5 GeV/c $< P_T^W <$ 10 GeV/c.

In this work, the $W^{\pm}$ kinematics was, for the first time, fully reconstructed for a spin observable, following the analysis techniques previously used at the Tevatron and LHC experiments; see, e.g., Ref. [18]. In reconstructing the boson kinematics, the momentum of the neutrino produced in the leptonically decayed $W \to l + \nu$ can only be deduced indirectly from transverse momentum conservation: $\vec{P}_T^{W} = -\vec{P}_T^{\text{recoil}}$. At the STAR detector, because of its limited pseudorapidity acceptance, the challenge with measuring the momentum from the hadronic recoil is that particles at high pseudorapidities are not detected. However, particles at high pseudorapidity typically carry only a small fraction of the total transverse momentum. The unmeasured tracks and clusters are accounted for by using an event-by-event Monte Carlo (MC) correction to the data. The correction factor c_i to the measured W transverse momentum in the i-th bin is defined as

$$c_i = \frac{P_{T,i}^{W}(\text{true})}{P_{T,i}^{\text{recoil}}(\text{reconstructed})}, \tag{2}$$

where $P_{T,i}^{W}(\text{true})$ is the P_T of the W generated by the MC calculations and $P_{T,i}^{\text{recoil}}$ (reconstructed) is the P_T of the recoil reconstructed in each i-th bin after a full simulation of the detector and applying all of the selection requirements. For each event, the measured value of the boson P_T was corrected by randomly sampling a value from the corresponding P_T bin of the normalized correction factor distribution.

In identifying the hadronic recoil from the tracks and clusters, events are rejected if the total $P_T^{\text{recoil}} < 0.5$ GeV/c, a region where the correction factor becomes large and has a broad distribution. The MC simulation using PYTHIA 6.4 [19] with the "Perugia 0" tune [20] shows that, after the correction has been applied, the reconstructed P_T of the W boson agrees with the independent prediction from RhicBOS [21], as shown in Fig. 1. The MC samples have been passed through the GEANT 3 [22] simulation of the STAR detector and are embedded into events from a zero-bias trigger.

Knowing its transverse momentum, the longitudinal component of the neutrino's momentum, P_L^{ν}, can be reconstructed, solving the quadratic equation for the invariant mass of the produced boson,

$$M_W^2 = (E_e + E_\nu)^2 - (\vec{P}_e + \vec{P}_\nu)^2, \tag{3}$$

where the nominal value of the W mass is assumed. Equation (3) leads to two possible solutions for P_L^{ν}. A MC study showed that for $|P_L^{\nu}| < 50$ GeV/c, corresponding to a W boson rapidity $|y^W| < 0.6$, the solution with the smaller absolute value gives, on average, a more accurate reconstruction of the originally generated W boson kinematics.

Potentially significant background sources in this analysis are $Z^0 \to e^+e^-$; $W^{\mp} \to \tau^{\mp}\bar{\nu}_\tau \to e^{\mp}\bar{\nu}_e\bar{\nu}_\tau$, where one of the final leptons is not detected; and events with an underlying two-to-two parton scattering (QCD events). The first two sources have been evaluated using MC

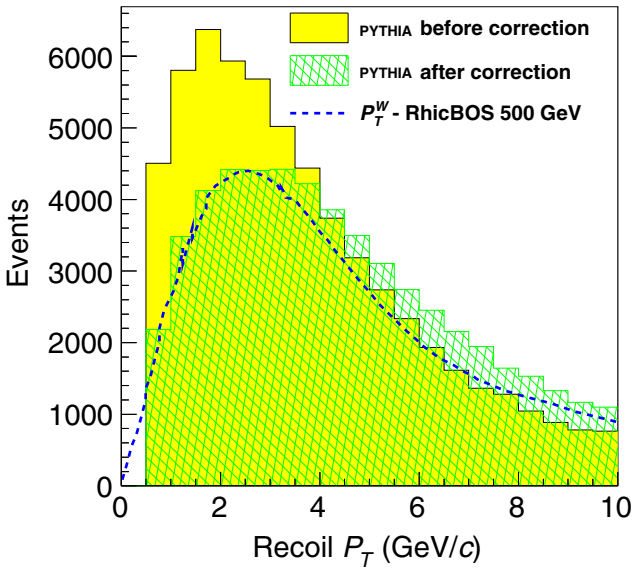

FIG. 1. P_T^{recoil} distribution of events simulated with PYTHIA 6.4 and reconstructed before (yellow) and after (hatched green) the P_T correction has been applied is compared with predictions from RhicBOS (dashed blue).

TABLE I. Background (B) over signal (S) in the W^+ and W^- samples, respectively.

Process	$W^{\mp} \to \tau^{\mp}\bar{\nu}_{\tau}$	$Z^0 \to e^+e^-$	QCD
W^+ (B/S)	$1.89\% \pm 0.04\%$	$0.79\% \pm 0.03\%$	$1.6\% \pm 0.09\%$
W^- (B/S)	$1.77\% \pm 0.10\%$	$2.67\% \pm 0.10\%$	$3.39\% \pm 0.23\%$

samples simulated with PYTHIA 6.4 using the Perugia 0 tune. To estimate the relative contribution from background, the MC samples have been normalized to the W^+ and W^- data samples according to the collected luminosity. In estimating the background from QCD events, we adopted the same "data-driven" technique used in previous STAR publications on $W^{\pm}$ production [16,17], reversing the selection criterion on $(\vec{P}_T^{\,\mathrm{bal}} \cdot \vec{P}_T^{\,e})/|\vec{P}_T^{\,e}|$ in order to select a data sample dominated by the background. All background sources have been estimated to be, at most, a few percent of the selected sample, as reported in Table I and shown in Fig. 2.

In the present work, A_N was also measured for Z^0 production, which is expected to be of the same magnitude [23] as for the $W^{\pm}$ boson and equally sensitive to the sign change of the Sivers function. The Z^0 bosons have a background with negligible impact on the spin asymmetry measurement and the kinematics is easily reconstructed from the two decay leptons produced within the acceptance of the STAR detector. Thus, the measurement is very clean and carries only the overall systematic uncertainty arising from the polarization measurement. The only experimental challenge is the much lower cross section of the $Z^0 \to e^+e^-$ process, leading to poor statistics. The $Z^0 \to e^+e^-$ events have been selected to require two electrons with $P_T > 25$ GeV/c, of opposite charge, and with an invariant

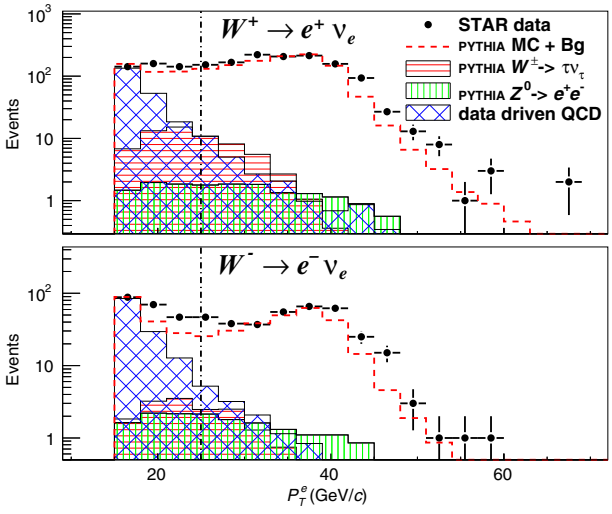

FIG. 2. Estimated background contributions are shown for the W^+ (upper panel) and the W^- (lower panel) data samples, respectively. A vertical line marks the minimum P_T^e value in this analysis.

mass within $\pm 20\%$ of the Z^0 mass value. Only 50 events remained after applying all of the selection criteria.

For each y^W and P_T^W bin, the data sample was divided into eight bins of the azimuthal angle ϕ of the produced boson, and the amplitude A_N of the $\cos(\phi)$ modulation was extracted by fitting the following distribution, which to first order cancels out false asymmetries due to geometry and spin-dependent luminosity differences [24]

$$A_N = \frac{1}{\langle P \rangle} \frac{\sqrt{N_{\uparrow}(\phi)N_{\downarrow}(\phi+\pi)} - \sqrt{N_{\uparrow}(\phi+\pi)N_{\downarrow}(\phi)}}{\sqrt{N_{\uparrow}(\phi)N_{\downarrow}(\phi+\pi)} + \sqrt{N_{\uparrow}(\phi+\pi)N_{\downarrow}(\phi)}}, \tag{4}$$

where N is the number of W^+, W^-, or Z^0 events reconstructed in collisions with an up or down ($\uparrow/\downarrow$) beam polarization orientation, and $\langle P \rangle$ is the average beam polarization magnitude. Defininning the up transverse spin direction $\vec{S}_{\perp}$ along the y axis and the direction of the polarized beam $\vec{p}_{\mathrm{beam}}$ along the z axis, the azimuthal angle is defined by $\vec{S}_{\perp} \cdot (\vec{P}_T^W \times \vec{p}_{\mathrm{beam}}) = |\vec{P}_T^W| \cdot \cos(\phi)$.

The results for A_N in W^+ and W^- production are shown in Fig. 3 (for details see Ref. [25]) as a function of P_T^W (the upper-left plot) and the W rapidity, y^W (the bottom plots). The absolute resolution in each of the three y^W bins has been estimated to be ~0.2–0.3, whereas the relative resolution on P_T^W decreases from ~50% in the first bin down to ~30% in the last bin. The systematic uncertainties, shown separately by the shaded error bands in Fig. 3, have been evaluated through a MC method. Events simulated by PYTHIA have been reweighted with asymmetries calculated according to EIKV [8] as a function of P_T^W and y^W. The systematic uncertainties are obtained comparing the generated and reconstructed distributions. The 3.4% scale uncertainty on the beam polarization measurement is not shown in the plots.

For the Z^0 production, because of the low counts in the sample, A_N was extracted for a single y^Z, P_T^Z bin, following the same procedure used for the $W^{\pm}$, as shown in Fig. 3 (upper-right plot). The solid gray bands in Fig. 3 (lower panels) represent the uncertainty due to the unknown sea quark Sivers functions estimated by saturating the sea quark Sivers function to their positivity limit in the Kang-Qiu (KQ) [11] calculation.

This analysis has yielded first measurements of a transverse spin asymmetry for weak boson production. The A_N results as a function of y^W, shown in Fig. 3 (bottom plots), are compared with theory predictions from KQ, which does not account for TMD evolution, and from Echevarria-Idilbi-Kang-Vitev (EIKV) [8]. The latter is an example among many TMD-evolved theoretical calculations (see, e.g., Ref. [26]), though EIKV predicts the largest effects of TMD evolution among all current calculations. Therefore, the hatched area in Fig. 3 represents the current uncertainty in the theoretical predictions accounting for TMD

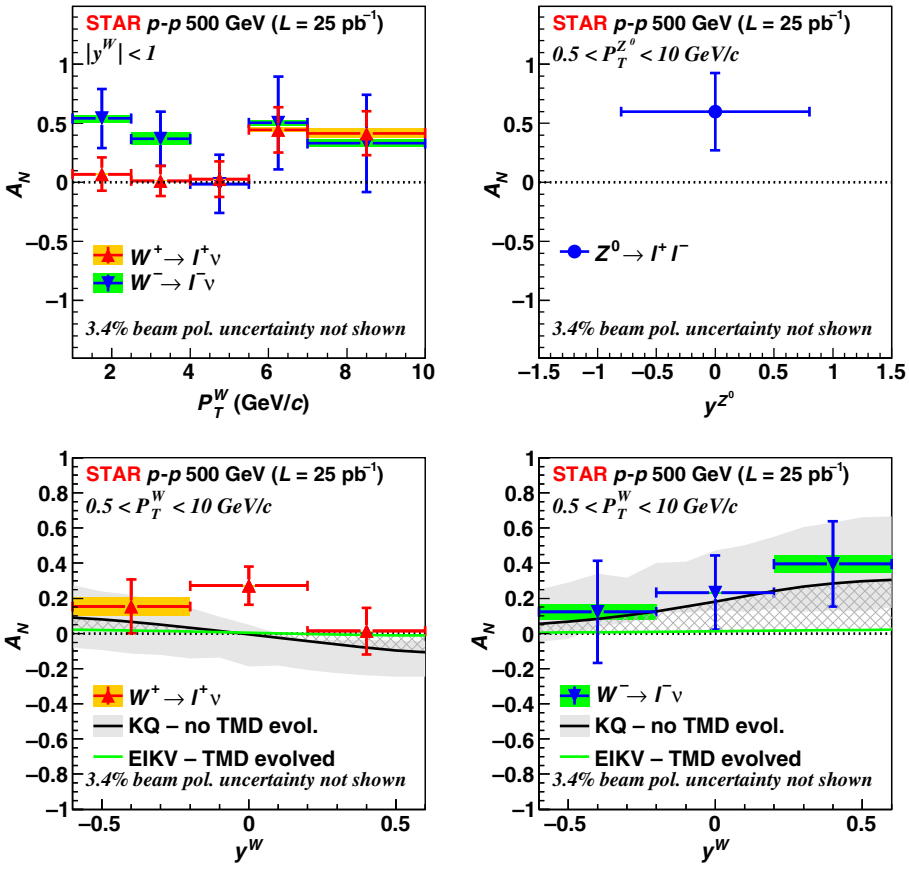

FIG. 3. The amplitude of the transverse single-spin asymmetry for $W^{\pm}$ and Z^0 boson production measured by STAR in proton-proton collisions at $\sqrt{s} = 500$ GeV, with a recorded luminosity of 25 pb^{-1}. The solid gray bands represent the uncertainty on the KQ [11] model due to the unknown sea quark Sivers function. The crosshatched region indicates the current uncertainty in the theoretical predictions due to TMD evolution.

evolution. In contrast to the Dokshitzer-Gribov-Lipatov-Altarelli-Parisi (DGLAP) [27] evolution used for collinear parton distribution functions, TMD evolution contains, in addition to terms directly calculable from QCD, also nonperturbative terms, which need to be determined from fits to experimental data. A consensus on how to obtain and handle the nonperturbative input in the TMD evolution has not yet been reached [28]; therefore, the results presented

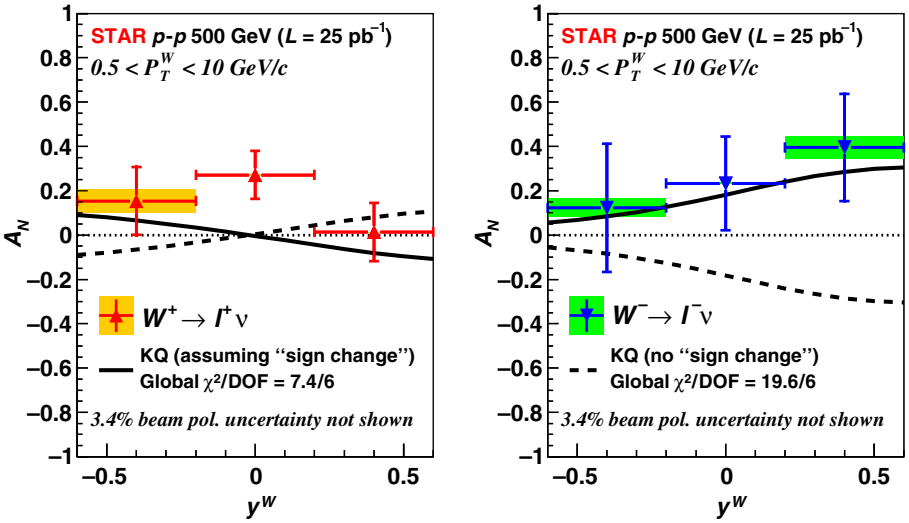

FIG. 4. Transverse single-spin asymmetry amplitude for W^+ (left plot) and W^- (right plot) versus y^W compared with the non-TMD-evolved KQ [11] model, assuming (solid line) or excluding (dashed line) a sign change in the Sivers function.

here can help to constrain theoretical models. A combined fit on W^+ and W^- asymmetries, $A_N(y^W)$, to the theoretical prediction in the KQ model (with no TMD evolution), shown in Fig. 4, gives a $\chi^2/\mathrm{DOF} = 7.4/6$, assuming a sign change in the Sivers function (the solid line) and a $\chi^2/\mathrm{DOF} = 19.6/6$ otherwise (the dashed line). The current data thus favor theoretical models that include a change of sign for the Sivers function relative to observations in SIDIS measurements, if TMD evolution effects are small.

We are grateful to Z.-B. Kang for the useful discussions. We thank the RHIC Operations Group and RCF at BNL, the NERSC Center at LBNL, the KISTI Center in Korea, and the Open Science Grid consortium for providing resources and support. This work was supported in part by the Office of Nuclear Physics within the U.S. DOE Office of Science, the U.S. NSF, the Ministry of Education and Science of the Russian Federation, NNSFC, CAS, MoST and MoE of China, the National Research Foundation of Korea, GA and MSMT of the Czech Republic, FIAS of Germany, DAE, DST, and UGC of India, the National Science Centre of Poland, National Research Foundation (NRF-2012004024), the Ministry of Science, Education and Sports of the Republic of Croatia, and RosAtom of Russia.

[1] S. Mert Aybat and T. C. Rogers, Phys. Rev. D **83**, 114042 (2011).
[2] S. Meissner, A. Metz, and M. Schlegel, J. High Energy Phys. 08 (2009) 056.
[3] D. W. Sivers, Phys. Rev. D **41**, 83 (1990); **43**, 261 (1991).
[4] A. Airapetian *et al.* (HERMES Collaboration), Phys. Rev. Lett. **94**, 012002 (2005); M. Alekseev *et al.* (COMPASS Collaboration), Phys. Lett. B **673**, 127 (2009); X. Qian *et al.* (Jefferson Lab Hall A Collaboration), Phys. Rev. Lett. **107**, 072003 (2011).
[5] J. C. Collins, Phys. Lett. B **536**, 43 (2002).
[6] S. J. Brodsky, D. S. Hwang, and I. Schmidt, Phys. Lett. B **530**, 99 (2002); Nucl. Phys. **B642**, 344 (2002); X. Ji and F. Yuan, Phys. Lett. B **543**, 66 (2002).
[7] Nuclear Science Advisory Committee, 2007 Long Range Plan, Milestone HP13, http://science.energy.gov/np/nsac/.
[8] M. G. Echevarria, A. Idilbi, Z.-B. Kang, and I. Vitev, Phys. Rev. D **89**, 074013 (2014).
[9] E. A. Hawker *et al.*, Phys. Rev. Lett. **80**, 3715 (1998).
[10] A. Metz and J. Zhou, Phys. Lett. B **700**, 11 (2011).
[11] Z.-B. Kang and J.-W. Qiu, Phys. Rev. Lett. **103**, 172001 (2009).
[12] RHIC Polarimetry Group, RHIC/CAD Accelerator Physics Note No. 490, 2013, http://public.bnl.gov/docs/cad/Documents/RHIC%20polarization%20for%20Runs%209-12.pdf.
[13] K. H. Ackermann *et al.* (STAR Collaboration), Nucl. Instrum. Methods Phys. Res., Sect. A **499**, 624 (2003).
[14] M. Anderson *et al.* (STAR Collaboration), Nucl. Instrum. Methods Phys. Res., Sect. A **499**, 659 (2003).
[15] M. Beddo *et al.* (STAR Collaboration), Nucl. Instrum. Methods Phys. Res., Sect. A **499**, 725 (2003).
[16] L. Adamczyk *et al.* (STAR Collaboration), Phys. Rev. Lett. **113**, 072301 (2014); M. M. Aggarwal *et al.* (STAR Collaboration), Phys. Rev. Lett. **106**, 062002 (2011).
[17] L. Adamczyk *et al.* (STAR Collaboration), Phys. Rev. D **85**, 092010 (2012).
[18] D. Acosta *et al.* (CDF Collaboration), Phys. Rev. D **70**, 032004 (2004); G. Aad *et al.* (ATLAS Collaboration), J. High Energy Phys. 12 (2010) 060; S. Chatrchyan *et al.* (CMS Collaboration), J. High Energy Phys. 10 (2011) 132.
[19] T. Sjöstrand, S. Mrenna, and P. Skands, J. High Energy Phys. 05 (2006) 026.
[20] P. Z. Skands, Phys. Rev. D **82**, 074018 (2010).
[21] P. M. Nadolsky and C.-P. Yuan, Nucl. Phys. **B666**, 3 (2003); **B666**, 31 (2003).
[22] R. Brun, F. Carminati, and S. Giani, CERN Report No. W5013, 1994.
[23] Z.-B. Kang (private communication).
[24] S. Bültmann *et al.*, Phys. Lett. B **632**, 167 (2006); **647**, 98 (2007); G. G. Ohlsen and P. W. Keaton, Jr., Nucl. Instrum. Methods **109**, 41 (1973).
[25] See Supplemental Material http://link.aps.org/supplemental/10.1103/PhysRevLett.116.132301 for the data depicted in Fig. 3.
[26] S. M. Aybat, A. Prokudin, and T. C. Rogers, Phys. Rev. Lett. **108**, 242003 (2012); M. Anselmino, M. Boglione, and S. Melis, Phys. Rev. D **86**, 014028 (2012); P. Sun and F. Yuan, Phys. Rev. D **88**, 114012 (2013).
[27] G. Altarelli and G. Parisi, Nucl. Phys. **B126**, 298 (1977); Yu. L. Dokshitzer, Sov. Phys. JETP **46**, 641 (1977); V. N. Gribov and L. N. Lipatov, Sov. J. Nucl. Phys. **15**, 438 (1972).
[28] J. Collins, EPJ Web Conf. **85**, 01002 (2015).